Journal of Thermal Analysis and Calorimetry, Vol. 91 (2008) 3, 929–936

POLYMERIC AND SANDWICH SCHIFF'S BASES COMPLEXES DERIVED FROM 4,4'-METHYLENEDIANILINE
Characterization and thermal investigation

S. A. AbouEl-Enein[*]

Chemistry Department, Faculty of Science, Menoufia University, Shebin El-Kom, Egypt

Cobalt(II), nickel(II) and copper(II) complexes of Schiff's bases derived from 4,4'-methylenedianiline and pyridine-2-carboxaldehyde(L^1), furan-2-carboxaldehyde(L^2) or thiophene-2-carboxaldehyde(L^3), were prepared and characterized by different analytical and spectral methods. The Schiff bases behave as neutral tetradentate ligands. The chloro-complexes of (L^2) with (2:3) mole ratio have a polymeric nature. However, that of L^1 and L^3 with (1:1) mole ratio showed a sandwich structure. All complexes display an octahedral geometry, except complex (2) which has a tetrahedral one. O_h/T_d equilibrium for chloro-complexes of cobalt with ligand L^1 was established in the solid state. ESR spectra of solid copper(II) complexes showed isotropic and axial type with $dx^2–y^2$ ground state. The thermal study showed that the complexes with different solvents of crystallization exercise different types of interaction. The observed thermochromic phenomenon for cobalt complex was explained along with its thermal behaviour.

Keywords: *4,4'-methylenedianiline (MDA), polymeric metal complexes, Schiff's bases, thermal analysis, thermochromic*

Introduction

4,4'-methylenedianiline, known as diaminodiphenyl methane (MDA), is used as intermediate in the manufacture of polyurethane foams. It is also used as a curing agent for epoxy resins, urethane elastomers, a corrosion preventative for iron, antioxidant for lubricating oils, rubber processing and preparation of azo-dyes [1, 2]. MDA is a hazardous substance that causes liver damage, skin and eye irritation [1–3]. On the other hand, it was reported that some Schiff bases of aniline derivatives display anti-inflammatory and antipyretic properties. These properties increased with copper(II) complexes [4]. Bis-(4-aminophenyl-methane) salicylaldehydeimine ligand and its metal complexes were also synthesized and characterized [5]. The complexes were found to be active against some microorganisms.

In the present work, metal complexes of different Schiff's bases of 4,4'-methylenedianiline with pyridine-2-carboxaldehyde, furan-2-carboxaldehyde or thiophene-2-carboxaldehyde were prepared and characterized. This was carried out in an attempt to investigate the effect of donor atoms (N,O,S) in hetero-rings on the coordination mode of the ligand. The metal complexes obtained were characterized by different analytical and spectral methods. The thermal behaviours of some metal complexes obtained were also investigated.

Experimental

Materials

All the chemicals used were reagent grade (BDH or Aldrich). Schiff's bases were prepared by addition of 4,4'-methylenedianiline (MDA) to pyridine-2-carboxaldehyde (L^1) I, furan-2-carboxaldehyde (L^2) II or thiophene-2-carboxaldehyde (L^3) III in (1:2) molar ratio in ethanol. The reaction mixture was stirred in air at 50°C for 30 min. The formed precipitate was

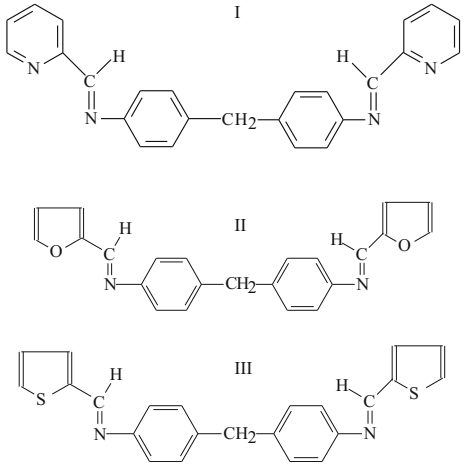

Scheme 1 I – Bis-[4-benzylidene-pyridine-2'-yl] methane (L^1), II – Bis-[4-benzylidene-furan-2'-yl] methane (L^2), III – Bis-[4-benzylidene-thiophene-2'-yl] methane (L^3)

* dr.saeyda_elenein@yahoo.com

1388–6150/$20.00

Akadémiai Kiadó, Budapest, Hungary
Springer, Dordrecht, The Netherlands

Table 1 Colors, elemental analysis results, magnetic moments (B.M.) and molar conductivities of the prepared metal complexes

No.	Compound	Color	Found (Calc.)/%				Λ_M^a	μ_{eff} (B.M.)
		FW	C	H	N	M		
	L^1	Yellow	80.00	5.30	14.50	–	–	
	$C_{25}H_{20}N_4$	376.47	(79.80)	(5.35)	(14.9)	–		
1	$[Co_2L^1_2Cl_4]\cdot 6H_2O\cdot 0.5EtOH$	Brown	53.76	4.92	9.80	10.30	48	4.60
	$C_{51}H_{55}Cl_4Co_2N_8O_{6.5}$	1143.8	(53.56)	(4.85)	(9.80)	(10.30)		
2	$[Co_2L^1_2]\cdot Cl_4\cdot 8H_2O$	Green	51.46	4.66	9.49	9.80	173	4.33
	$C_{50}H_{56}Cl_4Co_2N_8O_6$	1156.8	(51.91)	(4.90)	(9.69)	(10.20)		
3	$[Ni_2L^1_2Cl_4]\cdot 9H_2O\cdot EtOH$	Dark brown	51.77	5.29	9.00	9.50	5.19	3.11
	$C_{52}H_{64}Cl_4Ni_2N_8O_{10}$	1220.34	(51.18)	(5.29)	(9.18)	(9.62)		
4	$[Ni_2L^1_2Cl_4]\cdot 10H_2O$	Reddish brown	50.09	5.06	9.20	10.00	5.04	3.2
	$C_{50}H_{60}Cl_4Ni_2N_8O_{10}$	1191.94	(50.38)	(5.07)	(9.40)	(9.82)		
5	$[Cu_2L^1_2Cl_4]\cdot 2H_2O\cdot 2EtOH$	Dark brown	56.38	4.83	9.10	10. 90	27.5	1.75
	$C_{54}H_{56}Cl_4Cu_2N_8O_4$	1150.03	(56.40)	(4.90)	(9.70)	(11.04)		
6	$[Cu_2L^1_2Cl_4]\cdot 7H_2O$	Yellowish green	52.32	4.77	9.46	10.80	29.1	2.12
	$C_{50}H_{54}Cl_4Cu_2N_8O_7$	1148.12	(52.31)	(4.74)	(9.76)	(11.06)		
	L^2	Yellow	77. 80	5.00	7.60	–	–	
	$C_{23}H_{18}N_2O_2$	354.41	(77. 90)	(5.00)	(7.90)			
7	$[Co_2L^2_3]_n\cdot(Cl_4\cdot H_2O\cdot EtOH)_n$	Brown	61.60	4.9	6.30	8.30	–	4.90
	$(C_{71}H_{62}Cl_4Co_2N_6O_8)_n$	1387.10	(61.48)	(4.50)	(6.00)	(8.50)		
8	$[Ni_2L^2_3]_n\cdot(Cl_4\cdot 2EtOH)_n$	Brown	62.80	5.30	6.23	7.75	–	3.28
	$(C_{71}H_{62}Cl_4Ni_2N_6O_8)_n$	1414.20	(62.00)	(4.70)	(5.90)	(8.27)		
9	$[Cu_2L^2_3]_n\cdot(Cl_4\cdot 6H_2O\cdot EtOH)_n$	Dark brown	57.31	5.10	5.65	8.60	–	1.02
	$(C_{71}H_{72}Cl_4Cu_2N_6O_{13})_n$	1486.2	(57.38)	(4.88)	(5.70)	(8.55)		
	L^3	Yellow	71.80	4.80	7.20	–	–	
	$C_{23}H_{18}N_2S_2$	386.41	(71.50)	(4.70)	(7.00)			
10	$[Ni_2L^3_2Cl_4]\cdot 6H_2O\cdot EtOH$	Pale yellow	48.62	4.50	4.28	9.40	39.9	3.05
	$C_{48}H_{54}Cl_4Ni_2N_4S_4O_7$	1185.8	(48.62)	(4.59)	(4.72)	(9.87)		
11	$[Cu_2L^3_2Cl_4]\cdot 2EtOH$	Dark brown	53.30	4.40	4.80	11.30	50.1	0.99
	$C_{50}H_{48}Cl_4Cu_2N_4S_4O_2$	1133.92	(53.00)	(4.30)	(4.90)	(11.21)		

FW: Formula mass, *M*: Metal analysis, Λ_M: Molar conductance in 10^{-3} M DMF, *a*: Ohm^{-1} mol^{-1} cm^2, μ_{eff} (B.M.) per metal ion

filtered off, washed with ethanol several times and dried. The general structures of ligands obtained, from elemental analyses and spectral methods, are given in Scheme 1.

Co(II), Ni(II) and Cu(II) complexes of all ligands were prepared by the addition of 0.02 mole of the metal chloride dissolved in ethanol to a hot ethanol solution of 0.01 mole of ligand. The reactants were stirred for 2 h at 70°C. The precipitates obtained were filtered off, washed with ethanol and dried in vacuum and stored in a desiccator over $CaCl_2/P_4O_{10}$ for two weeks. The complexes of pyridine derivative (L^1) (1, 3, 5) were prepared by the same method in (1:1) mole ratio.

Methods

The elemental analyses were performed using a Perkin-Elmer C H N 2400 elemental analyzer. Metal analyses were carried out complexometrically [6, 7].

IR spectra were recorded using KBr discs on a Perkin-Elmer 1430 spectrophotometer. Electronic absorption spectra were recorded as Nujol mulls using Perkin-Elmer Lambda-4B spectrophotometer. Room temperature magnetic susceptibility measurements were carried out on a modified Gouy-type magnetic balance, Herts SG8-5HJ. Diamagnetic correction was done using Pascal constants [8]. The molar conductivity was measured for (10^{-3}M) DMF solutions using a Tacussel conductometer type CD6N.

Thermal analyses (DTA/TG) were measured in a stream of nitrogen atmosphere within the temperature range (25–1000°C) using a Shimadzu DTA/TG – 50 with a heating rate of 10°C min^{-1}. The flow rate of N_2 was 10 cm^3 min^{-1}. The mass of the investigated samples was 0.9718–5.6740 mg. ESR spectra were recorded at 100 kHz-modulation and 4G-modulation amplitude on variation using ESR spectrophotometer (Bruker Model EMX) at the National Center of Researches and Radiation Technology, Egypt.

Results and discussion

All the complexes are stable and non-hygroscopic. The metal complexes of the furan-derivative are insoluble in most organic solvents. This behaviour could be attributed to the polymeric nature of the complexes [9]. The metal complexes of pyridine and thiophene derivatives are soluble in DMF. The molar conductivity values of the soluble complexes in DMF (Table 1) indicate nonelectrolytic nature [10, 11], except for the green cobalt complex (2). The molar conductivity value of that complex is 176 mol^{-1} cm^2, typified 1:2 electrolyte [12].

Infrared spectra

The spectra of the ligands show a band within the range 1598–1627 cm^{-1} which is assigned to υ(C=N) of azomethine group [10, 13]. The spectra also display other bands near 1628, 1357–1282 and 717–700 cm^{-1} assigned to pyridine ring, furan ring stretching and υ(C–S–C), respectively [14, 15]. The pyridine, furan and thiophene ring bending vibration appeared at (637, 582, 516, 483), (637, 582) and (566, 444, 430) cm^{-1}, respectively [14]. The spectra of all complexes display bands in the range 3560–3342 cm^{-1} due to υ(H_2O) [7, 16, 17]. The observed low frequency shift of υ(C=N) for all complexes relative to that of the corresponding free ligand is due to the participitation of azomethine group in coordination. The spectra are also characterized by a new band in range 408–527 cm^{-1} assigned to υ(M–N) [15, 18]. The spectrum of the pyridine ligand (I) complexes showed changes in position and shape of pyridine ring bending in/out of the plane at 637, 583 and 516, 483 cm^{-1} and pyridine ring at 1628 cm^{-1}. This is attributed to the participitation of pyridyl nitrogen atom in the coordination with metal ion. For the furan ligand (II) complexes, the furan ring bending band at 582 cm^{-1} was shifted to high frequency by 5–10 cm^{-1} on complexation. Also, the strong furan ring stretching bands at 1357 and 1280 cm^{-1} suffer from changes (in both shape and position) on complexation. The first peak shifted to lower frequency by 26 cm^{-1} whereas the second one weakened. This indicates the participitation of oxygen atom of furan ring in coordination. The coordination through oxygen atom of furan ring was also confirmed by the appearance of a medium new band at 506–555 cm^{-1} which is assigned to υ(M–O) [15, 19, 20]. For thiophene ligand (III) complexes, the spectrum showed that the thiophene ring stretching bands at 1519 and 1500 cm^{-1} suffer from low frequency shifts on complexation. The υ(C–S–C) of free ligand gave a low frequency shift by a value of 20 cm^{-1}. Also, thiophene ring bending vibration at 566 cm^{-1} displayed a positive/negative shift whereas that at 440 cm^{-1} disappeared on complexation. This indicates the participitation of sulphur atom in complexation [15].

Electronic spectra

Electronic spectra and room temperature magnetic moment are measured, from their values the following can be pointed out.

Cobalt complexes

The green cobalt(II) complex (2) showed intense multicomponent band with maxima at 620, 632, 668 and 704 nm. This band is assigned to tetrahedral configuration around the metal ion [21]. This assignment was also confirmed by the value of magnetic moment (μ_{eff}=4.33 B.M.). The spectra of complexes (1 and 7) display a strong band at 416–422 nm and another weak splitted band at 624–710 nm. These bands gathered with the μ_{eff} value (4.6–4.9 B.M) indicate an octahedral geometry [21, 22].

Nickel complexes

The spectra of nickel(II) complexes gave three bands in the ranges 336–382, 404–488 and 698–716 nm, indicating an octahedral geometry [4, 23]. The room temperature magnetic moment values in the range (μ_{eff} =3.05–3.28 B.M.) are consistent with the octahedral geometry [24, 25].

Copper complexes

The spectra of copper(II) complexes display bands at 338–356, 428–464, 524–584 and 680–712 nm. These bands are assigned to tetragonally distorted octahedral structure [26]. The geometry obtained was also confirmed by the values of μ_{eff}. The observed lower magnetic moment values for complexes 9 and 11 (μ_{eff} 0.996, 1.023 B.M) may be attributed to Cu–Cu interaction, due to the crystal packing in the solid state [5, 26].

The room temperature solid powder (ESR) data of copper(II) complexes showed that complexes (5, 6 and 11) are of isotropic behaviour with g=2.10, 2.07 and 2.08, respectively. These values confirm an octahedral geometry with covalent bonding [27]. Copper(II) complex (9) gave anisotropic symmetry with two g-values, g_{11}=2.2 and $g_{\perp}$=2.06. The data show $g_{11}>g_{\perp}>g_e$ confirming a $dx^2–y^2$ ground state in a distorted octahedral geometry [26, 28]. The G value is a measure of the exchange interaction between copper centers in polycrystalline solid. If G>4 exchange interaction is negligible and if G<4 considerable exchange interaction occurred in the solid complex. Complex (9) gave G value=3.3, indicating the presence of exchange coupling [29].

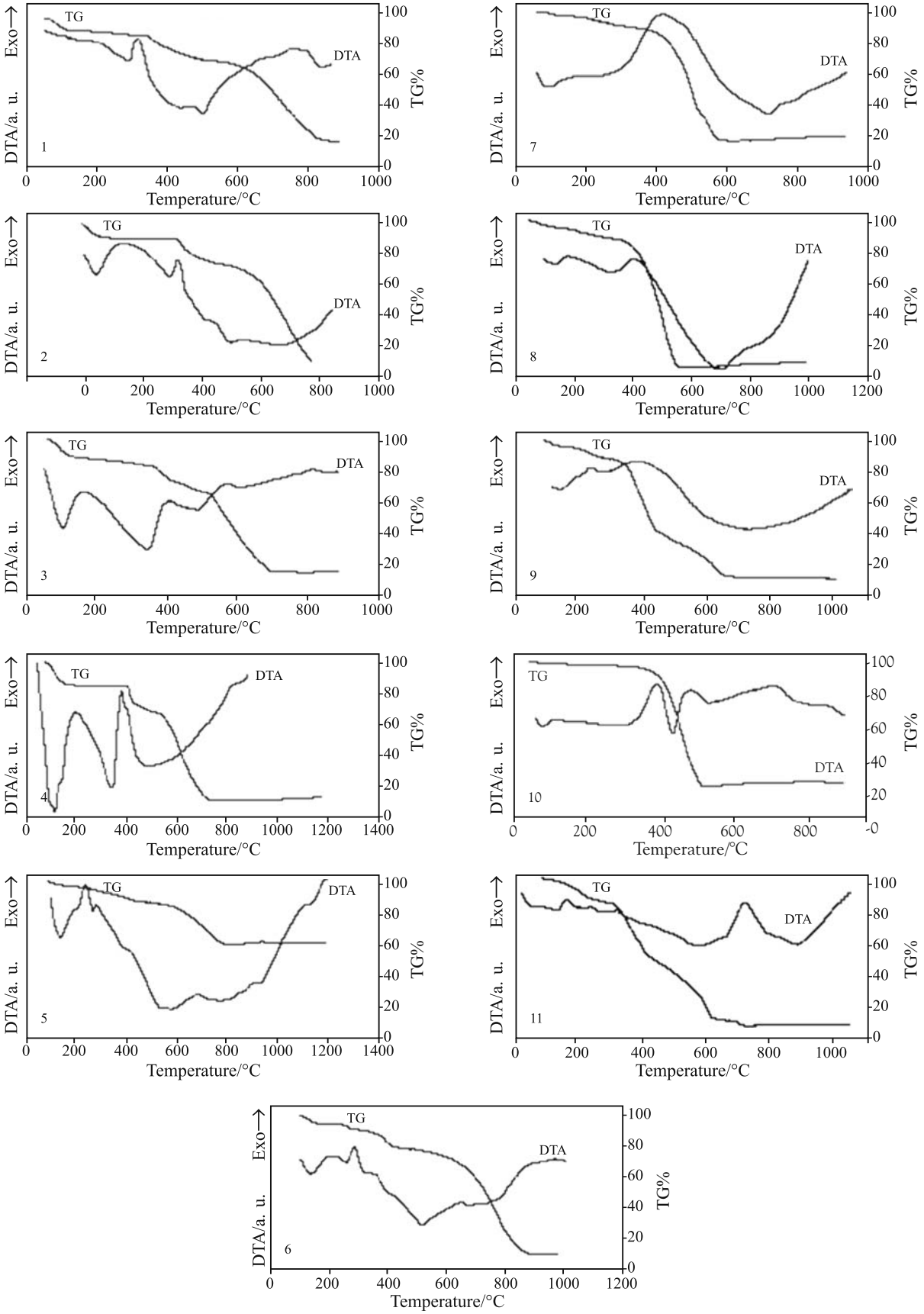

Fig. 1 DTA/TG curves for metal complexes

Table 2 Thermal analysis (DTA/TG) data for the metal complexes

No.	Compound	DTA Peak/ °C	Temp. range/°C		Mass loss Found (Calc.)/ %	Reaction	Assignment*	T_s/ °C
			DTA	TG				
1	$[Co_2L^1_2Cl_4]\cdot 6H_2O\cdot 0.5EtOH$	endo (63.34)	29–169.2	29–169.2	9.71 (9.63)	$6H_2O$	a	304
		shoulder end o	169.2–250	169.2–250	1.98 (2.01)	0.5EtOH	b+ green form	
		endo (274)	250–304	250–304	–	phase change	Oh brown – Td green	
			850	304–437	12.66 (12.41)	4Cl atoms	c	
				437–850	61.20 (61.63)	2MDA, 20C, $6H_2$, $2N_2$	c remain	
				850	14.43 (14.50)	2Co+4C		
2	$[Co_2L^1_2]\cdot Cl_4\cdot 8H_2O$	endo (64.6)	29–157.1	29–157.1	9.5 (9.34)	$6H_2O$	a	332
		endo (305)	157.1–332.9	157.1–332.9	–	lattice rearrangement		
				332–462.2	15.62 (15.39)	4Cl atoms, $2H_2O$	c	
			322–462.2					
		endo (504.7), endo (690.6)	462–542.3, 542.3–803	462–542.3, 542–803	65.09 (65.09)	2 molecules of ligand	c	
				803	(9.76) (10.18)	2 Co	remain	
3	$[Ni_2L^1_2Cl_4]\cdot 9H_2O\cdot EtOH$	endo (77.3)	25–130	25–130	12.50 (12.62)	$6H_2O$, EtOH	a, b	345
		endo (170)	130– 369	130–345, 345–369	10.36 (10.24)	$3H_2O$, 2Cl atoms	a and c	
		endo (470)	369–555	369 –555	25.40 (25.24)	2Cl atoms, 3-pyridine rings	c	
		endo (600)	555–750	555–725	38.34 (38.25)	2 diphenylmethane, 5N, 5C, H	c	
				750°	13.14 (13.55)	2Ni+4C	remain	
4	$[Ni_2L^1_2Cl_4]\cdot 10H_2O$	endo (98.2)	28–180	28–180	15.36 (15.10)	$10H_2O$	a	364
		endo (334)	180–364	180–364	–	lattice rearrangement		
		shoulder	364–410	364–410	11.80 (11.90)	4Cl atoms	c	
		endo (480)	410–725	410–725	57.91 (58.12)	$2N_2$, 2MDA, 19C, $6H_2$	c	
				725	14.85 (14.88)	2Ni+5C	remain	
5	$[Cu_2L^1_2Cl_4]\cdot 2H_2O\cdot 2EtOH$	endo (67.14)	20–116	20–116	5.70 (5.57)	H_2O, EtOH	a, b	177
		shoulder (143.2)	116–177	116–177	1.63 (1.57)	H_2O	a	
			177–390	177–390	16.35 (16.35)	EtOH, 4Cl atoms	b, c	
		endo (532), endo (752)	390–650 650–820	390–772	60.61 (60.24)	2MDA, 19C, $6H_2$, $2N_2$	c	
				772	15.71 (16.27)	2Cu+5C	remain	
6	$[Cu_2L^1_2Cl_4]\cdot 7H_2O$	endo (63.06)	23–120,	23–120,	7.70 (7.80)	$5H_2O$	a	212
		endo (187.5)	120–212	120–212				
		shoulder	212–250, 250–350	212–350	12.25 (12.36)	4Cl atoms	c	
		endo (463), endo (633) shoulder	350–544 544–650 650–855	350–814	65.78 (65.93)	2 ligand, $2H_2$	c	
				818	13.37 (13.85)	2CuO	remain	
7	$[Co_2L^2_3]_n\cdot (Cl_4\cdot H_2O\cdot EtOH)_n$	endo (61.7)	27–146	27–146	3.46 (3.33)	EtOH	b	146
		exo (379.4)	146–670	i) 146–365.7	11.27 (11.53)	H_2O,4Cl atoms	a,c	
				ii) 365.7–470	51.0 (51.10)	2 ligand	c	
				iii) 470–611	23.54 (23.24)	MDA, 10C	c	
				611	10.73 (10.80)	2CoO	remain	
8	$[Ni_2L^2_3]_n\cdot (Cl_4\cdot 2EtOH)_n$	endo (56)	25–117	25–117	5.75 (5.67)	1.75 EtOH	b	117
		endo (256)	117–339	117–339	10.9 (10.85)	4Cl atoms,0.25EtOH	c	
				339–561	75.7 (75.10)	3 ligands		
				561	7.65 (8.27)	2Ni	remain	

Table 2 Continued

No.	Compound	DTA Peak/ °C	Temp. range/°C DTA	Temp. range/°C TG	Mass loss Found (Calc.)/ %	Reaction	Assignment	T_s/ °C
9	$[Cu_2L^2_3]_n \cdot (Cl_4 \cdot 6H_2O \cdot EtOH)_n$	endo (61.88)	31–165	31–165	6.41 (6.42)	$2.75H_2O$, EtOH	a, b	209
		endo (219)	165–309	i)165–209	3.92 (3.94)	$3.25H_2O$	a	
				ii) 209–309	9.24 (9.55)	4Cl atoms	c	
		endo (692)	309–1044	309–670	72.06 (71.54)	3 ligands	c	
				670	8.37 (8.55)	2Cu	remain	
10	$[Ni_2L^3_2Cl_4] \cdot 6H_2O \cdot EtOH$	endo (48.0), (115)	28–74, 74–138	28–74, 74–138	1.96 (1.89)	$1.25H_2O$	a	369
		endo (288.4)	138–369	138–369	4.32 (4.26)	$0.25H_2O$,EtOH	a, b	
		endo (413)	369–469	369–511	77.95 (78.58)	2MDA, $4.5H_2O$, 4Cl, 10C, $2H_2$	c	
				511	15.77 (15.23)	2NiS	remain	
11	$[Cu_2L^3_2Cl_4] \cdot 2EtOH$	endo(50.5), (127)	32–156	32–156	8.60 (8.23)	2EtOH	b	156
		endo (209), (245)	156–236	156–236	6.00 (6.20)	2Cl	c	
			236–304	236–304	10.38 (10.36)	Cl, 4C,2S	c	
				304–594	60.50 (60.74)	2DMA, 6C, 2 thiophene	c	
		exo 716	567.5–772	594–704	3.16 (3.13)	Cl		
				704	11.36 (11.50)	2Cu	remain	

*a – dehydration, b – desolvation, c – decomposition, T_s – decomposition temperature

Thermal studies

DTA and TG curves of the investigated metal complexes (1–11) are given in Fig. 1. The results of thermal analysis together with their assignments are also given in (Table 2). It was found that all metal complexes are thermally stable up to 48°C and the complexes lose their solvents of crystallization in one or multi-steps. The endothermic dehydration and/or desolvation process are generally extended over a broad temperature range 25–369°C [30–32] and sometimes overlap with the decomposition step for complexes (2, 3, 5, 7, 9 and 10). The dehydration peak is followed by an endo- or exothermic peak which is assigned to decomposition process. As derived from TG mass loss (Table 2), the general mechanism for decomposition of chloro-complexes started with the elimination of chloride atoms [32, 33]. This may be attributed to the weak nature of metal chloride bond relative to other bonds in molecule. This step was followed by the decomposition or removal of the organic ligands. The solid residue of thermal decomposition (Table 2) are metal [34, 35], metal oxide [36, 37], metal sulphide [38] or a mixture of metal and carbon [5, 21]. DTA curve of the brown cobalt(II) complex (1) (Fig. 1) gave an endothermic peak in the temperature range 29–169°C. This peak is assigned to loss of six molecules of water of crystallization as derived from TG mass loss (Table 2). This endothermic dehydration peak was followed by another endothermic peak (shoulder) in the temperature range 169–250°C corresponding to the loss of 0.5 EtOH. DTA curve also display an endothermic peak near 250–304°C. This peak is assigned to thermochromic phase change from brown into dark green one [21, 32]. This assignment was confirmed by TG data which show no mass loss in that temperature range. This thermochromic phase change is reversible through (1 h) in the solid state and may take place through chloride ion exchange between ionisable and coordination spheres, giving an octahedral (brown form)/tetrahedral (green form) transformation [21]. This type of transformation was derived from electronic spectral measurements of both brown and green forms. The green form displays a similar spectrum to that of tetrahedral green complex (2). Complex (1) also shows a similar thermochromic behaviour in hot DMF solution where the brown octahedral form change into tetrahedral green one. Such transformation is also reversible on cooling as in the solid state. The observed lower magnetic moment value of both brown and green forms (4.6 and 4.33 B.M) may be attributed to some type of equilibrium between both forms in the solid state. DTA curve also displays a number of endothermic peaks in the temperature range 304–850°C that may be assigned to thermal decomposition of complex to give a mixture of cobalt metal and carbon as a final product. This assignment was also confirmed by TG mass loss (Ta-

$$[Co_2L^1_2Cl_4] \cdot 6H_2O \cdot 0.5EtOH \xrightarrow{29-169\,^\circ C} [Co_2L^1_2Cl_4] \cdot 0.5EtOH \xrightarrow{169-250\,^\circ C} [Co_2L^1_2Cl_4]$$

brown O_h loss $6H_2O$ brown O_h loss 0.5 EtOH

$$[Co_2L^1_2Cl_4] \xrightarrow{250-304\,^\circ C} [Co_2L^1_2] \cdot Cl_4 \xrightarrow{304-850\,^\circ C} 2Co + 4C$$

phase change dark green decomposition

ble 2). The thermal behaviour of the complex can be represented as follows:

DTA curve of green tetrahedral cobalt(II) complex (2) (Fig. 1) gave two successive endothermic peaks near 64 and 305°C. These peaks are assigned to dehydration and lattice rearrangement [5, 32], respectively as derived from TG mass loss (Table 2). TG curve displays a mass loss (9.5%) in the temperature range 29–157°C corresponding to six molecules of water. No mass loss was observed in the temperature range 157–333°C, confirming the lattice rearrangement assignment [32]. Those two endothermic peaks were also followed by other endothermic peaks in the temperature range 333–803°C, assigned to material decomposition to give finally cobalt metal. The observed higher thermal stability of the green form up to (333°C) than that of brown form (304°C) may be attributed to the increased number of water molecules of crystallization which play an effective role in the lattice forces [39].

As shown in DTA/TG curves (Fig. 1) of reddish brown and dark brown nickel(II) complexes, the complexes loss their solvent of crystallization through endothermic (one or two steps) process. The reddish brown form (4) changes into a dark brown one in the temperature range 180–364°C through an endothermic lattice rearrangement. This lattice rearrangement was derived from TG measurements which show no mass loss in that temperature range (Table 2). This thermal behaviour is similar to a great extent to that of its room temperature isostructural cobalt(II) complex (1).

TG and DTA curves of isostructural copper(II) complexes of pyridine derivatives (5, 6) are given in Fig. 1. Both complexes display a number of endothermic splitted DTA peaks in the temperature range 25–212°C. These peaks are assigned to loss of some solvents of crystallization as derived from TG mass losses. The endothermic desolvation peaks are followed by a number of endothermic/exothermic events that are assigned to material decomposition to give finally (Cu+C) and CuO for complexes (5) and (6), respectively. It is noteworthy to mention that the yellowish green form of, complex (6) changes to a dark brown one, (5) on heat treatment in the solid state or dissolution in DMF.

The polymeric nickel(II) and copper(II) complexes of ligand II (8, 9) largely exhibit similar thermal behaviours (Fig. 1). This is due to their isostructural character at room temperature. The observed endothermic DTA peaks together with the corresponding TG mass losses (Table 2) are assigned to desolvation as well as material decomposition. The decomposition proceeds via rupture of coordinate bond by elimination of three ligand molecules along with dechlorination to give nickel and copper metals as final products. As shown in Table 2 and Fig. 1, the DTA curve of complex (7) displays an endothermic peak at 61.7°C which is assigned to loss of one EtOH molecule corresponding to mass loss of 3.33%. The exothermic decomposition takes place through dechlorination as well as loss of the two ligand molecules in the temperature rang 146–611°C. The final product of decomposition is CoO as derived from TG mass loss.

The DTA curves of nickel and copper complexes (10, 11) display endothermic peaks in the temperature range 28–369°C, assigned to dehydration / or desolvation as indicated from TG mass loss (Table 2). The thermal decomposition of complexes takes place through successive endothermic/exothermic processes within the temperature range 156–772°C. As derived from TG mass loss, the decomposition proceeds via dechlorination and ligand molecules loss in accordance with the general behaviour of the other investigated complexes. The final products are NiS and Cu metal for complex (10) and (11), respectively.

The observed lower thermal stability of copper complexes of ligands I and III than those of cobalt and nickel complexes may be attributed to the higher repul-

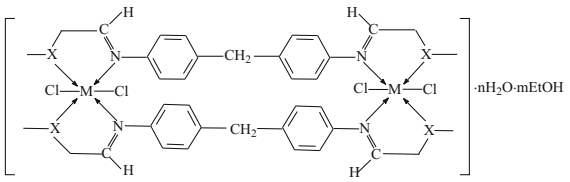

Complex	*M*	*n*	*m*
1	Co (II)	6	0.5
3	Ni (II)	8	1
4	Ni (II)	10	–
5	Cu (II)	2	2
6	Cu (II)	7	–
10	Ni (II)	6	1
11	Cu (II)	–	2

X: represents N or S atom of pyridine ring (1-6) or thiophene ring (10, 11)

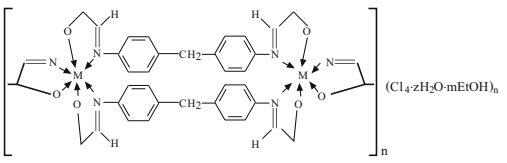

Complex	*M*	*Z*	*m*
7	Co (II)	1	1
8	Ni (II)	–	2
9	Cu (II)	6	1

Scheme 2

sion between bonding pair of electrons in the valence shell of copper ion relative to those of cobalt and nickel [40]. Also, the complexes of ligand II generally display lower thermal stability than those of ligands I and III. This may be related to the steric hindrance around the metal ion in the polymeric complexes of ligand II.

On basis of the above discussion together with elemental analyses and TG measurements, the structures in Scheme 2 can be suggested, for the studied metal complexes.

Conclusions

Metal complexes of Schiff's base ligands derived from 4,4'-methylenedianiline and pyridine, furan or thiophene-2-carboxaldehyde were prepared and investigated. DTA and TG studies of complexes obtained display the following points:

- The general mechanism for decomposition of chloro-complexes started with the elimination of chloride followed by the decomposition or removal of organic ligands.
- The thermal stability is controlled by the metal ion type and steric effect of the ligands.
- Cobalt(II) complex, (1) displays a reversible thermochromic phase change in the solid state and in DMF solution.

References

1 U. S. Environmental Protection Agency, Health and Environmental Effects Profile for Benzenamine, 4,4' Methylenebis . EPA/ 600/x – 84/231, Cincinnati OH. 1984.
2 The Merck Index, An Encyclopedia of Chemicals, Drugs and Biological 11th ed. Ed. S. Budavari. Merck and Co. Inc. Rahway, NJ. 1989.
3 S. S. Que Hee, Proceeding of International Conference on Occupational and Environmental Exposure Skin to Chemicals, Hilton Crystal City Sept. 8–11 (2002), p. 1.
4 R. K. Parashar, R. C. Sharma, K. Anil and M. Govind, Inorg. Chim. Acta, 151 (1988) 201.
5 A. S. El-Tabl, J. Chem. Res., Issue (S) (2002) 529.
6 G. Schwarzenback, 'Complexmetric Titration', Transl. by H. Irving, Muth. Uen. Co., London 1957.
7 T. Premkumar and S. Govindarajan, J. Therm. Anal. Cal., 84 (2006) 395.
8 P. W. Selwood, 'Magnetochemistry', Interscience Publisher Inc., New York 1956.
9 T. Prermkumar, S. Govindarajan, W. P. Pan and R. Xie, J. Therm. Anal. Cal., 74 (2003) 325.
10 H. M. El-Tabl, F. A. El-Saied and M. I. Ayad, Synth. React. Inorg. Met.-Org. Chem., 32 (2002) 1247.
11 O. E. Sherif, H. M. Abd EL-Fattah and M. M. El-Ajily, J. Therm. Anal. Cal., 74 (2003) 181.
12 F. H. Urěna, N. A. I.-Cebeza, M. N. M.-Carretero, J. M. M.-Martos and M. J. R.-Exposito, J. Inorg. Biochem., 94 (2003) 326.
13 R. Olar, M. Badea, E. Cristurean, V. Lazar, R. Cernet and C. Balotescu, J. Therm. Anal. Cal., 80 (2005) 451.
14 J. B. Lambert, H. F. Shurvell, L. Verbit, R. G. Cooks and G. H. Stout, Organic Structural Analysis, Macmillan Publishing Co., Inc, New York 1976.
15 G. G. Mohamed, M. M. Omar and A. M. M. Hindy, Spectrochim. Acta, A62 (2005) 1140.
16 E. C. Rodrigues, A. B. Siqueira, E. Y. Ionashiro, G. Bannach and M. Ionashiro, J. Therm. Anal. Cal., 79 (2005) 323.
17 B. K. Singh, R. K. Sharma and B. S. Garg, J. Therm. Anal. Cal., 84 (2006) 593.
18 G. Singh and D. K. Pandey, J. Therm. Anal. Cal., 82 (2005) 353.
19 M. Tas and H. Bati, J. Therm. Anal. Cal., 85 (2006) 295.
20 W. Brzyska and W. Ozga, J. Therm. Anal. Cal., 84 (2006) 385.
21 H. A. El-Boraey, J. Therm. Anal. Cal., 81 (2005) 339.
22 I. Labádi, L. Horváth, G. Kenessey and G. Liptay, J. Therm. Anal. Cal., 83 (2006) 247.
23 A. B. P. Lever, Inorganic Electronic Spectroscopy, 2nd. Edn., Elsevier, Amsterdam 1984.
24 W. Ferenc, B. Bocian and J. Sarzynski, J. Therm. Anal. Cal., 84 (2006) 377.
25 I. Labadi, G. Kenessey and G. Liptay, J. Therm. Anal. Cal., 82 (2005) 55.
26 M. S. Masoud, S. A. AbouEl-Enein, M. E. Aayd and A. S. Goher, Spectrochim. Acta, A60 (2004) 77.
27 A. S. El-Tabl, Trans. Met. Chem., 27 (2002) 166.
28 K. Narang and V. P. Singh, Trans. Met. Chem., 21 (1996) 507.
29 A. S. El-Tabl, Bull. Korean Chem. Soc., 25 (2004) 1757.
30 P. Masset, J. Y. Poinso and J. C. Poignet, J. Therm. Anal. Cal., 83 (2006) 457.
31 M. S. Refat, I. M. El-Denn, H. K. Ibrahim and S. El-Ghool, Spectrochim. Acta, A65 (2006) 1208.
32 A. M. Donia and H. A. El-Boraey, J. Anal. Appl. Pyrol., 63 (2002) 69.
33 A. M. Donia, M. I. Ayad and R. M. Issa, Trans. Met. Chem., 16 (1991) 518.
34 A. M. Donia, H. A. El-Boraey and M. F. El-Samalehy, J. Therm. Anal. Cal., 73 (2003) 987.
35 B. Kebede, N. Retta, V. J. T. Raju and Y. Chebude, Trans. Met. Chem., 31 (2006) 19.
36 R. Olar, M. Badea, E. Cristurean, C. Parnau and D. Marinescu, J. Therm. Anal. Cal., 84 (2006) 53.
37 H. A. El-Boraey, A. M. Donia and M. F. El-Samalehy, J. Anal. Pyrol., 73 (2005) 204.
38 Z. B. Leka, V. M. Leovac, S. Lukic, T. J. Sabo, S. R. Trifunovic and R. M. Szecsenyi, J. Therm. Anal. Cal., 83 (2006) 687
39 M.S. Masoud, A. Khalil, E. El-Shereafy and S. A. El-Enein, J. Thermal Anal., 36 (1990) 1033.
40 G. Mohamed and Z. H. Abdel-Wahab, J. Therm. Anal. Cal., 73 (2003) 347.

Received: November 27, 2006
Accepted: June 19, 2007

DOI: 10.1007/s10973-006-8281-z